

## Chapter 9

# Fluvial Processes: Meandering and Braiding

### 9.1 General

In general, *fluvial processes* that belong to the geomorphologic category cover the complete chronological processes of formation and evolution of a river system from where it originates to end up in an estuary. However, in a specific sense, fluvial processes that belong to the category of fluvial hydrodynamics focus on river morphological changes occurring due to natural processes and/or engineering activities, such as river regulation and training works. The fluvial processes of rivers are the result of the interaction of stream flow, sediment, and riverbed. The riverbed controls the flow and sediment transport, which in turn enhance changes in the riverbed. Thus, they are interdependent, but complement each other. The characteristics of rivers are related to the gradient of the terrain from extremely steep mountainous torrents to steep rivers at the foot-hills and rivers in the plains. Thus, a river could be regarded as it consisting of upper, middle, and lower reaches which correspond to erosion, regime, and aggradations states, respectively. In upper reach, the sediment transport capacity by the stream flow is generally greater than the prevailing sediment transport rate, leading to an erosion of the streambed. In middle reach, the sediment transport rate is less than the transport capacity by the stream due to gradual streambed armoring followed by a long-term bed-sorting process. This river reach is in a state of quiescent erosion or so-called regime. In lower reach, aggradations occur due to substantial reduction in transport capacity with decrease in valley slope.

According to the static and dynamic characteristics, alluvial river patterns are in general categorized as (1) straight, (2) meandering, and (3) braided rivers (Leopold and Wolman 1957):

1. *Straight rivers* have minimal *sinuosity*<sup>1</sup> ( $< 1.1$ ) at the bankfull conditions. Usually, rivers, as simple straight open channels, exist only over short reaches

---

<sup>1</sup> The ratio of the curvilinear length to the linear distance (straight line) between the end points of the curve is known as *sinuosity* or *sinuosity index*. In case of a river, it is the ratio of the actual river length to the down-valley length. Its minimum value is unity for a perfectly straight river.

(Fig. 9.1); while long, straight rivers seldom occur in nature. At low flow stages, alluvial bars exist on either side of the stream. The thalweg<sup>2</sup> may wind in a sinuous route along the bars, even though the channel is straight. The thalweg may move with alternate bars as they migrate downstream.

2. *Meandering rivers* (sinuosity  $> 1.5$ ) consist of a series of turns with alternate curvatures connected at the points of inflection or by short straight crossings, as shown in Figs. 9.2 and 9.3. They have a relatively low gradient. The natural meandering rivers are quite unstable due to predominant bank erosion downstream of concave banks. Deeper flows are prevalent in the bends and higher velocities along the outer concave banks. The flow depth at crossings is relatively shallow compared to that at bends. Meandering rivers migrate gradually and hence sinuosity tends to increase. Eventually, the channel forms almost a closed loop and the meander gets often cutoff during a flood. Meandering is therefore the result of streambed instability; in particular, when instability acts on the banks.

Here, it is pertinent to discuss that the rivers with a sinuosity of less than 1.1 is described as straight, those between 1.1 and 1.5 are *sinuous*, and meandering rivers have a sinuosity of greater than 1.5. Therefore, sinuous rivers are the transition between straight and meandering rivers. Although these descriptions are commonly used, they are somewhat arbitrary, since they are not based on any physical differences. Further, there is a tendency for the thalweg to swing from side to side along the rivers. This is observed even in straight rivers and is often associated with the development of riffles, pools, and alternate bars.

3. *Braided rivers* are wide and shallow and divided to branches by a number of semistable or unstable bars or islands (Figs. 9.4 and 9.5). More specifically, braided river can be defined as one that flows in two or more channels around alluvial bars or islands. They have a braided look at the low flow stages with exposed bars, but all or some of the bars are submerged during the high flow stages. However, in most of the occasions, the branching is such that one is the main stream and the others are subsidiary channels. The main stream is relatively stable, but it can change its route under some flow and sediment transport conditions, while the subsidiary channels are quite unstable and often change during floods.

In changing the planform geometry, that is the transition from meandering to braiding and vice versa, although it is best viewed as gradual, empirical equations were put forward to set up some potential relations for the threshold of meandering or braiding (Carson 1984). Leopold and Wolman (1957) gave a relationship to define the transition from meandering to braiding involving riverbed slope  $S_0$  and bankfull discharge  $Q_{bf}$  ( $\text{m}^3 \text{s}^{-1}$ )

---

<sup>2</sup> The locus of lowest bed elevation or maximum flow depth within a watercourse is known as *thalweg*.



**Fig. 9.1** Photograph of a straight river. Photograph by the author



**Fig. 9.2** Aerial photograph of a meandering river (courtesy of O. Link, Universidad de Concepción, Chile)

$$S_0 = 0.012Q_{bf}^{-0.44} \quad (9.1)$$

The above equation, which is the simplest one, indicates that the threshold bed slope above which a river could exhibit a braided form increases with a decrease in bankfull discharge. In addition, Lane (1957) proposed slightly different criterion for the thresholds of meandering from a straight river and braiding from a meandering river by using mean annual discharge  $Q$  as

$$\begin{aligned} S_0 &= 7 \times 10^{-4} Q^{-0.25} \text{ (meandering threshold),} \\ S_0 &= 0.004 Q^{-0.25} \text{ (braiding threshold)} \end{aligned} \quad (9.2)$$



**Fig. 9.3** Photograph of a meandering river. Photograph by the author



**Fig. 9.4** Photograph of a braided river downstream of a valley glacier (courtesy of O. Link, Universidad de Concepción, Chile)





**Fig. 9.5** Photograph of a braided river with gravel bars. Photograph by the author

The above equations are in metric units being applicable for sand-bed streams. Note that the bed slopes for these two thresholds (meandering and braiding) differ by a factor of approximately 6.

Equations (9.1) and (9.2) are too general. Henderson (1963) and Ferguson (1987) identified the importance of participation of sediment size  $d_{50}$  along with mean annual discharge  $Q$  in defining the threshold of braiding from meandering. Henderson and Ferguson suggested the following equations, respectively:

$$S_0 = 2 \times 10^{-4} d_{50}^{1.15} Q^{-0.44} \quad \text{and} \quad S_0 = 4.9 \times 10^{-3} d_{50}^{0.52} Q^{-0.21} \quad (9.3)$$

where  $d_{50}$  is in mm and  $Q$  is in  $\text{m}^3 \text{s}^{-1}$ .

Parker (1976) related planform geometry to a form parameter  $E$  as

$$E = \frac{S_e B}{\pi F r h} \quad \wedge \quad F r = \frac{U}{\sqrt{g h_d}} \quad (9.4)$$

where  $S_e$  is the energy slope,  $Fr$  is the flow Froude number,  $h$  is the flow depth,  $B$  is the average river width,  $U$  is the area-averaged flow velocity,  $g$  is the acceleration due to gravity, and  $h_d$  is the hydraulic depth. In the above equation, the parameters  $B$ ,  $h$ ,  $U$ , and  $h_d$  correspond to the bankfull conditions. The meandering corresponds to  $E < 1$  and braiding to  $E > 1$ .

On the other hand, Millar (2000) argued that the bank vegetation affects planform geometry of a river. He showed that the resistance to bank erosion is to increase the threshold bed slope for braiding from meandering. He introduced a bank sediment friction angle  $\phi_b$  in degrees in his equation. The  $\phi_b$  takes into account the effects of binding of bank sediment by the roots of bank vegetation, sediment packing, etc. He suggested

$$S_0 = 2 \times 10^{-4} \phi_b^{1.75} d_{50}^{0.61} Q_{bf}^{-0.25} \quad (9.5)$$

where  $d_{50}$  is in m and  $Q_{bf}$  is in  $\text{m}^3 \text{s}^{-1}$ . The value of  $\phi_b$  is approximately  $40^\circ$  for sparsely vegetated gravel banks, but it can be as high as  $80^\circ$  for heavily vegetated banks because of the grip made by the roots.

Hayashi and Ozaki (1978) proposed the criteria for the prediction of different planforms in terms of flow Froude number  $Fr$  and a nondimensional parameter  $\tilde{B} = (BS_0/h_d)$  by using the stability analysis as follows:

$$\left. \begin{aligned} Fr &\geq 3.16\tilde{B}^{0.5} \text{ (straight)} \\ 3.16\tilde{B}^{0.5} &\geq Fr \geq 2\tilde{B}^{0.5} \text{ (transition from straight to meandering)} \\ 2\tilde{B}^{0.5} &\geq Fr \geq \tilde{B}^{0.5} \text{ (coexistence of meandering and braiding)} \\ \tilde{B}^{0.5} &\geq Fr \text{ (braiding)} \end{aligned} \right\} \quad (9.6)$$

## 9.2 Meandering Rivers

In alluvial plains of lower reaches, the rivers normally develop a single-twisting course, termed *meander*, as already discussed in preceding section. The degree of meandering of a river is defined by the *sinuosity*, which is the ratio of centerline length to wavelength of meander. Note that the thalweg length is also considered instead of centerline length by some authors. The sinuosity is a function of valley slope or stream power. For a meandering river, sinuosity that is always greater than unity increases with valley slope, but it reverts close to unity when braiding forms.

Figure 9.6 illustrates an idealized planform of a meandering river. In reality, unlike the idealized illustration, alternating bends of a meandering river are rather quasi-regular. The down-valley axis  $x$  in a rectilinear coordinate system represents the centerline of the meandering planform downstream of the valley slope, while the sinuous axis  $n$  in a curvilinear coordinate system defines the centerline of the meandering path. Points of inflection for changing the curvatures (also called crossovers) are denoted by  $I_{-1}$ ,  $I_0$ ,  $I_1$ , and  $I_2$ . The deflection angle  $\theta$  is the angle that creates the meandering path at any location  $n$  with the down-valley axis. It changes continuously along the sinuous axis  $n$ . Note that  $\theta(n=0) = \theta_0$  is the maximum value of  $\theta$ . It is pertinent to mention that the radius of curvature of meandering path denoted by  $r_c$  is not constant for a given meandering bend, so a single value of  $r_c$  is somewhat subjective to define for the meandering bend. For instance, the  $r_c$  is minimum at the apex of the bend and maximum at the crossings. Besides, the meandering wavelength is denoted by  $\lambda_m$ , the meandering arc length (that is the length along the meandering path between two repeating points of inflection) by  $L$ , the meandering belt width by  $B_m$ , the meandering amplitude (or meander width) by  $a_m$ , and the average flow width by  $B$ .

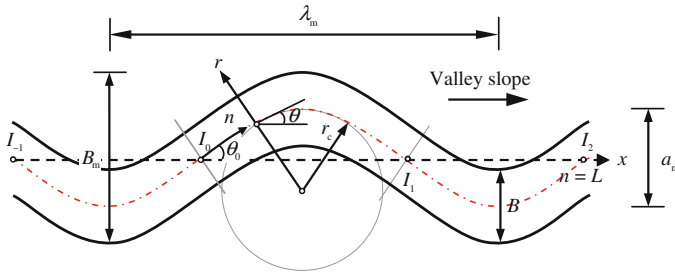


**Fig. 9.6** Definition sketch of an idealized planform of a meandering river

The idea of the *sine*-generated curve was used by von Schelling (1951) to outline the most probable path between fixed points. For a given number of steps, he considered the Gaussian distribution for the changing over the direction at the terminus of each step. He showed that a criterion for the most probable path of a continuous curve is obtained if the variance or overall curvature becomes a minimum. Following the minimum variance concept, Langbein and Leopold (1966) argued that a meandering river to achieve the minimum variance is more stable than a straight river and gave the equation of a regular meandering path as

$$\theta = \theta_0 \cos \frac{2\pi x}{L} \quad (9.7)$$

The above equation thus produces a *sine*-generated curve that can fit well the meandering path of a river, provided appropriate values of  $\theta_0$  and  $L$  are chosen.

In a meandering bend, the centrifugal acceleration influences the flow, which is characterized by a helical motion with a super-elevated free surface. Flow near the free surface is deflected toward the outer bank and near the bed is inclined toward the inner bank. This phenomenon is already discussed in Sect. 2.7. As a stream actively curves to flow, obvious erosion takes place at the outer bank (looking convex from the ground alongside the stream) of the bend. The sediment eroded from the outer bank is transported inward and deposited on the inner edge of the next bend downstream, where the flow velocity is slower, building up an inner point bar (Figs. 9.7 and 9.8). Remembering that the zone of high velocity in a meandering bend shifts from inner (at the inflection zone) to outer side (at the apex zone) with the distance, the zone of maximum bed shear stress shifts similar way. This effect actively shifts the river very slowly toward the eroded banks. The cross-section at the meandering bend apex is normally asymmetrical having deep portion of the stream located along the outer bank and a broad, shallow portion extending from the inner bank toward the center of the stream (Fig. 9.7). The thalweg wanders from deep pool at the outer side of a bend over a shallow crossover to next deep pool at the outer side of the next bend, and so on (Fig. 9.7). As most of the natural river sediments are nonuniform, the asymmetry in cross-section in meandering bends is associated with a spanwise sediment sorting feature. By the influence of the helicoidal flow, finer particles tend to move inward.

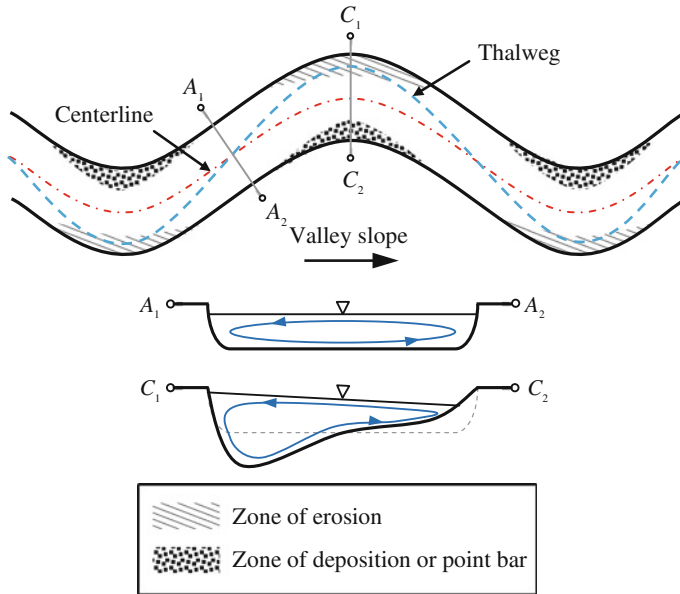


**Fig. 9.7** Sketch showing zones of erosion and deposition in a meandering river

In this way, the coarser particles tend to accumulate near the outer banks with a gradual fining toward the inner banks. Dietrich and Smith (1984) argued that the maximum flow depth is inversely proportional to the ratio of radius of curvature of the bend to stream width, that is,  $h_{\max} \sim (r_c/B)^{-1}$ . Note that the river that has a tendency to braiding does not have an exclusively localized erosion and deposition at the bends only. Evidently, the braiding occurs only when the stream power exceeds a higher threshold. Thus, the sequence of straight, meandering, and braided rivers corresponds to an increase in valley slope or stream power magnitude.

The meander loops are, in general, inherently asymmetrical due to local differences in bank erodibility producing irregularities in bend forms, although Langbein and Leopold (1966) tried to define them by a so-called *sine*-generated curve [see Eq. (9.7)]. In reality, the nature of this asymmetry in meander loops is not random, but they are well defined and somewhat consistent. Such an asymmetry to exist in meander loops does not appear to be the result of probability, but seems to reflect certain inherent flow features through bends. The most important feature in the asymmetrical meander loops is the location of the inflection points that alter on opposite sides of the valley axis, producing a *delayed inflection* from one meandering turn to the next one downstream (Carson and Lapointe 1983; Parker et al. 1983). Consequently, the most meandering bends are facing down-valley. Thus, from a geometric viewpoint, restraint of the meander amplitude could be at the expense of that part of the traverse downstream of the inflection point. In this process, it produces an aborted form that is dominantly convex





**Fig. 9.8** Photograph of a meandering river showing the erosion at outer banks and the formation of point bar in the inner bank (courtesy of L. Solari, University of Florence, Italy)



**Fig. 9.9** Photograph of the meandering loops of a river showing the potential of cutoff by the broken line (courtesy of Z. Wang, Tsinghua University, China)

down-valley. Delayed inflection is attributed to a delayed thalweg crossover leading to spatial variations of bank erosion rates being in turn translated into a delayed inflection in the meander loops. Note that the delayed inflection appears to be prevalent for the meandering rivers that carry considerable suspended load (Carson and Griffiths 1987).

Meander *cutoff* is a fundamental process in the evolution of meandering rivers. As the planform of a meandering river progressively migrates in the downstream direction and expands in the transverse direction, the meander loops shift at a differential rate due to nonuniform erosion rates at the banks. The resulting shape in a developed state appears to form a bulb with inflection zones of a loop to come closer forming a neck (two closest portions of river). Eventually, the banks at the neck breach by a chute channel, called *cutoff*, that connects the neck of the loop (Gagliano and Howard 1984; Hooke 1995). Figure 9.9 displays the potentiality of cutoff at the necks of meandering loops of a river. Besides bank-breaching, cutoff may also occur when floods incise a floodplain channel or chute that evolves into the dominant conveyor of river flow (Hooke 1995; Gay et al. 1998). The cutoff causes the flow to abandon the meander and to continue straight downslope. After formation of a cutoff, a new meandering bend may slowly grow again. Cutoffs are a natural part of the evolution of a meandering river. The abandoned meander forms an *oxbow lake* that may persist over a long time period before getting it filled. The oxbow lake formation process through a meandering neck cutoff is schematically illustrated in Fig. 9.10.

Ripley (1927) studied the meandering rivers and gave the criterion for a meander loop to have a tendency to form a cutoff as  $r_c < 40A^{0.5}$ , where  $A$  is the flow cross-sectional area. However, he also suggested the criterion for a stable meandering bend as  $40A^{0.5} < r_c < 110A^{0.5}$ .

The aforementioned description is related to sand-bed meandering rivers, which are regarded as low-energy rivers. Carson and Griffiths (1987) reported that the characteristics of gravel-bed meandering rivers, regarded as high-energy rivers, are considerably different from sand-bed rivers in terms of meandering outline. The gravel-bed rivers exhibit a *premature inflection* instead of a delayed inflection that is observed for a low-energy river. Premature inflection in high-energy rivers results in up-valley migration of meandering course and is associated with over-widening of meandering bends (Carson 1986). In low flow stages, high-energy meandering rivers sometimes have a tendency to cut across the point bars. This along with over-widening of meandering bends in low flow stages may initiate to develop the braiding. Carson and Griffiths (1987) designated this type of rivers' configuration, which is in fact a transition between meandering and braiding, as *pseudo-meandering streams*.

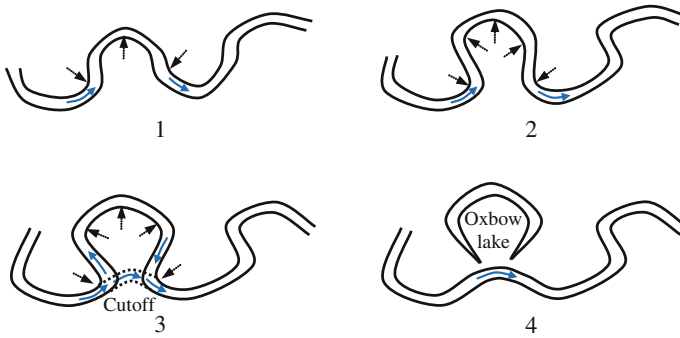


**Fig. 9.10** Oxbow lake formation process following a meandering loop cutoff shown in the sequence of 1–4 line diagrams

### 9.2.1 Meander Planform Characteristics

Field and laboratory observations on the dimensions of meandering geometry have been used to develop empirical relationships between certain planform characteristics that are somewhat consistent for a wide range of river sizes. Various investigators, importantly Inglis (1947), Leopold and Wolman (1957), and Zeller (1967), recognized that the meandering wavelength  $\lambda_m$  is directly proportional to flow width  $B$ . The relationship that was obtained by Garde and Ranga Raju (2000) from the data plots is

$$\lambda_m \approx 6B \quad (9.8)$$

Further, Leopold and Wolman (1960) proposed the following relationships between different planform characteristics of meandering rivers:

$$\lambda_m = 4.6r_c^{0.98}, L = 11B^{1.01}, a_m = 6B^{1.1} \quad (9.9)$$

The units of the quantities in Eq. (9.9) are in m.

On the other hand, Chang (1988) suggested  $r_c \approx 3B$ .

### 9.2.2 Concepts of Meandering

Attempts have been made to identify the cause of meandering and to understand the background mechanism of its development. Some of the important concepts are discussed below:

*Earth's Revolution Concept:* The *Coriolis effect*<sup>3</sup> is caused by the revolution of the earth, and the inertia of the mass of an object is to experience the effect. On the earth, an object that moves along a north–south path, or longitudinal line, undergoes apparent deflection to the right in the northern hemisphere and to the left in the southern hemisphere. Rather than rivers flowing directly as they would be in a nonrevolving system, the flow tends to the right in north of the equator and to the left in south of it. In the nineteenth century, naturalist Karl Ernst von Baer observed that the rivers in the northern hemisphere do most of their erosion on the side to the right of the direction of flow; and on the left in the southern hemisphere. The reason is attributed to the Coriolis effect. Albert Einstein (1926) simply observed that as the stream flow curves on the earth surface, the Coriolis effect induces rotational motion to the flow. The flow moves helicoidally downstream, as if a corkscrew moves. Einstein's discussion on the cause of meander was rather casual, but characteristically insightful, as his attribution of secondary currents to the Coriolis force might have been among the earliest. Besides, Gilbert (1884), Eakin (1910), and Lacey (1923) before Einstein's observation and Chatley (1938), Quraishy (1943), and Neu (1967) after Einstein's observation argued that the earth's revolution could be the cause of river meandering.

*Instability Concept:* Any irregularities or perturbations in the upstream flow cause a modification in the flow structure in the downstream direction leading to meandering. In fact, irregularities introduce instability to the flow and the bed to form meanders. The initial irregularities could be due to any obstacle or sediment deposition on the bed (Griggs 1906; Werner 1951), random velocity fluctuations due to turbulence (Hjulström 1957), oblique entry of flow in a channel (Friedkin 1945), or some other reasons. Agarwal (1983) observed alternate bars in an experimental flume by introducing a two-dimensional periodic disturbance on the bed.

*Helicoidal Flow Concept:* A group of investigators believed that the helicoidal flow due to secondary current of Prandtl's first kind (see Sect. 3.10) is potentially responsible for the occurrence of meandering. Since secondary current is present in all the stream flows, the asymmetry in secondary circulation due to asymmetrical cross-section and/or bed resistance of natural rivers is the cause to initiate meandering (Prus-Chacinski 1954; Leliavsky 1966; Onishi et al. 1976; Shen 1983). Once the meandering is initiated, secondary current of Prandtl's first kind is the governing mechanism.

*Excess Flow Energy Concept:* This concept is based on the energy content in the stream flow on which the meandering process is related. Flow in a meandering river is to reduce the excess energy (and in turn, to reduce the excess slope) of the flow by increasing its traveling length (Schoklitsch 1937; Inglis 1947). According to Bagnold, the energy loss in a bend is least if the ratio of bend radius to river width lies between 2 and 3. Based on Bagnold's concept of minimum bend loss,

---

<sup>3</sup> The *Coriolis effect* is an apparent deflection of the path of an object in motion due to an induced transverse force normal to its path, when it is set in a rotating reference frame. In a reference frame with clockwise rotation, the deflection is to the left of the motion of the object, while with counter-clockwise rotation, the deflection is to the right.

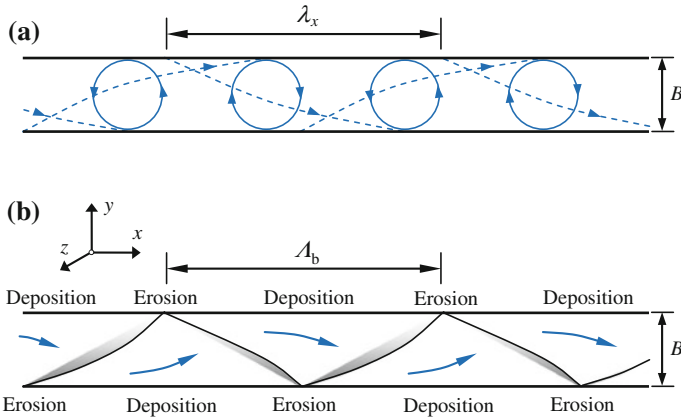


**Fig. 9.11** Conceptual illustration of large-scale eddy concept after Yalin and da Silva (2001): **a** top view of large eddies appearing at a relatively regular interval and **b** top view of alternate bars appearing at a relatively regular interval

Leopold and Wolman (1960) and Ramette (1980) argued that the minimization of energy is associated with the formation of meandering in rivers. However, Yang (1971) expressed dissatisfaction about the legitimacy of the hypothesis that a river meanders in order to dissipate excess flow energy. Thus, he introduced a concept of minimum time rate of energy expenditure. According to his concept, during the evolution of a meandering river toward its equilibrium state, a river finds its course of flow in such a way so that the minimum time rate of potential energy expenditure per unit mass of water prevails along its course.

*Large-Scale Eddy Concept:* Yalin and da Silva (2001) argued that the meandering is caused by the large-scale eddies. They identified that the horizontal length scale (streamwise spacing)  $\lambda_x$  of large eddies in a straight rectangular open channel approximately equals the horizontal length  $\lambda_b$  of alternate bars (Figs. 9.11a, b); and both the length scales are six times of the flow width  $B$ . The formation of alternate bars at a relatively regular interval is analogous to the formation of dunes caused by the large-scale eddies that also appear at a relatively regular interval resulting in decrease and increase in bed shear stress (see Fig. 8.4). Thus, taking into account the relationship given by Eq. (9.8), one can relate

$$\lambda_x = \lambda_b = \lambda_m \approx 6B \quad (9.10)$$

Equation (9.10) therefore suggests that both alternate bars and meanders initiate because of the same mechanism, that is, the large-scale eddies or large-scale turbulence structure. Alternate bars are caused by the action of large-scale turbulence structure collapse on the erodible bed, and the threshold of meandering is caused by the action of turbulence structure collapse on the erodible banks (Fig. 9.11b).



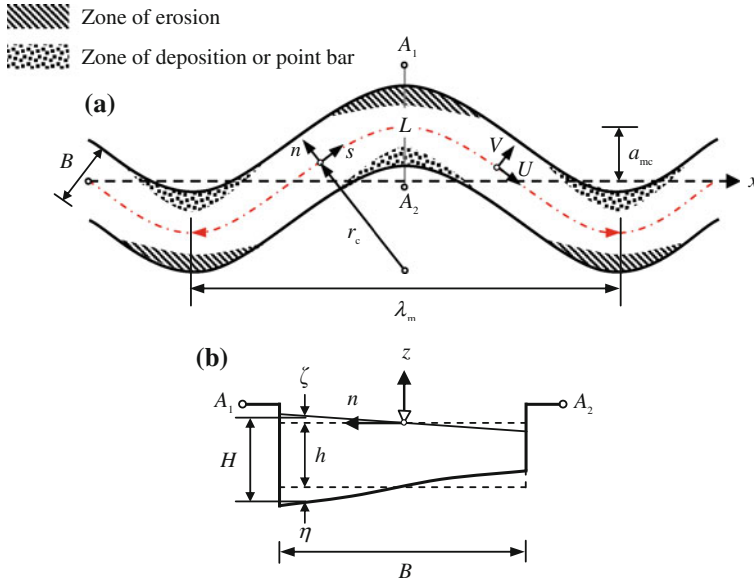


**Fig. 9.12** Definition sketch: **a** meandering river with coordinate system and **b** cross-section of river at  $A_1$ – $A_2$

### 9.3 Mathematical Modeling of Meandering Rivers

In this section, the flow and bed topography models developed by Ikeda and Nishimura (1986) and Odgaard (1989) are presented in details.

#### 9.3.1 Ikeda and Nishimura's Model

##### 9.3.1.1 Flow Field

Ikeda and Nishimura (1986) considered orthogonal curvilinear coordinates  $(s, n)$  to represent depth-averaged velocity components  $(U, V)$  (Fig. 9.12a). The  $U$  and  $V$  are decomposed as

$$U = \bar{U} + U', \quad V = V' \quad (9.11)$$

where  $\bar{U}$  is the reach-averaged velocity in  $s$ -direction, and  $U'$  and  $V'$  are the perturbed velocity components.

Referring to Fig. 9.12b, the average flow depth  $H$  is decomposed as

$$H = h + \zeta + \eta \quad (9.12)$$

where  $h$  is the reach-averaged flow depth,  $\zeta$  is the super-elevation of the free surface due to curvilinear flow induced by centrifugal inertia, and  $\eta$  is the change of bed elevation with respect to mean bed level due to erosion or deposition.

According to Kikkawa et al. (1976), the  $\eta$  is

$$\frac{\eta}{h} = \left(\frac{r}{r_c}\right)^{\vartheta} - 1 \quad \wedge \quad \vartheta = \left[\frac{3}{4} \cdot \frac{\mu C_D}{1 + \eta_R \mu}\right]^{0.5} \frac{\xi_s}{\kappa} \cdot \frac{\bar{u}_*}{(\Delta g d_{50})^{0.5}} \left(\frac{4.167}{\lambda_f^{0.5}} - 6.6\right) \quad (9.13)$$

where  $r = r_c + n$ ,  $\vartheta$  is an exponent defining erosion factor,  $\mu$  is the coefficient of dynamic viscosity,  $C_D$  and  $C_L$  are the drag and lift coefficients, respectively,  $\xi_s$  is the sheltering coefficient,  $\eta_R$  is  $C_L/C_D$ ,  $\kappa$  is the von Kármán constant,  $\bar{u}_*$  is the shear velocity at the centerline  $[= (ghS_0)^{0.5}]$ ,  $\Delta$  is the submerged relative density,  $\lambda_f$  is the friction parameter  $(= ghS_0/\bar{U}^2 = gh^3S_0/q^2)$ , and  $q$  is the discharge per unit width.

Using Eq. (9.13) and approximation of  $r_c$  by a *sine*-generated curve  $[r_c^{-1} = r_{c0}^{-1} \cos(k_{wb}s)]$ , perturbed streamwise velocity  $U'$  can be obtained as follows (Ikeda et al. 1981):

$$\frac{U'}{\bar{U}} = \frac{n}{r_{c0}} [a \sin(k_{wb}s) + b \cos(k_{wb}s)] \quad (9.14)$$

where  $r_{c0}$  is the minimum radius of curvature at the bend apex,  $k_{wb}$  is the wave number of centerline of meandering, and  $a$  and  $b$  are as follows:

$$a = \frac{\lambda_f k_{wb} h (\vartheta + Fr^2 + 2)}{4\lambda_f^2 + (k_{wb}h)^2}, \quad b = \frac{2(\vartheta + Fr^2)\lambda_f^2 - (k_{wb}h)^2}{4\lambda_f^2 + (k_{wb}h)^2} \quad \wedge \quad Fr = \frac{\bar{U}}{(gh)^{0.5}} \quad (9.15)$$

The wave number in meandering rivers, according to Ikeda et al. (1981), is expressed as  $k_{wb} = 1.5\lambda_f/h$ .

The perturbed transverse velocity  $V'$  is given by

$$\frac{V'}{\bar{U}} = \frac{k_{wb}r_{c0}}{2} \cdot \frac{r_c}{r} \cdot \frac{h}{H} [a \cos(k_{wb}s) - (b + \vartheta + Fr^2) \sin(k_{wb}s)] \left[ \left(\frac{B}{2r_{c0}}\right)^2 - \left(\frac{n}{r_{c0}}\right)^2 \right] \quad (9.16)$$

Assuming that the velocity defect law is preserved in streamwise velocity distributions in meandering rivers, the time-averaged streamwise velocity  $\bar{u}(z)$  at any elevation  $z$  was obtained by Ikeda and Nishimura. It is

$$\frac{\bar{u}}{\bar{u}_*} = \varphi \frac{U}{\bar{U}} \left[ \frac{\bar{U}}{\bar{u}_*} + \frac{1}{\kappa} (1 + \ln \hat{\eta}) \right] = \varphi \frac{U}{\bar{U}} \left[ \frac{1}{\lambda_f^{0.5}} + \frac{1}{\kappa} G(\hat{\eta}) \right] \quad \wedge \quad \hat{\eta} = 1 + \frac{z}{H} \quad (9.17)$$

where  $\varphi$  is a function of  $\hat{\eta}$  being unity in main flow zone and zero at the banks,  $G(\hat{\eta}) = 1 + \ln \hat{\eta}$ , and  $z$  is the vertical distance (Fig. 9.12b).

Then, centrifugally induced time-averaged transverse velocity component  $v''(z)$  of the secondary current is given by

$$\frac{v''}{U} = \varphi^2 \left( \frac{U}{\bar{U}} \right)^2 \frac{H}{\kappa r} \chi \varphi_0 \frac{r_c}{r_{c0}} \cos(k_{wb}s - \sigma_L) \quad (9.18)$$

where  $\chi$  is the factor for secondary current,  $\varphi_0 = \varphi_1(\hat{\eta}) - \lambda_f^{0.5} \kappa^{-1} \varphi_2(\hat{\eta})$ ,  $\varphi_1(\hat{\eta}) = -15(\hat{\eta}^2 \ln \hat{\eta} - 0.5 \hat{\eta}^2 + 0.278)$ ,  $\varphi_2(\hat{\eta}) = 7.5(\hat{\eta}^2 \ln^2 \hat{\eta} - \hat{\eta}^2 \ln \hat{\eta} + 0.5 \hat{\eta}^2 - 0.352)$ , and  $\sigma_L$  is the phase lag of the secondary current relative to meandering planform.

The vorticity equation for secondary current in a sinuous river is expressed as

$$\bar{u} \frac{\partial \Omega_s}{\partial s} - \frac{2}{r} \bar{u} \frac{\partial \bar{u}}{\partial z} = \varepsilon_t \frac{\partial^2 \Omega_s}{\partial z^2} \quad \wedge \quad \Omega_s \approx \frac{\partial v''}{\partial z} \quad (9.19)$$

where  $\Omega_s$  is the vorticity of secondary current, which is approximated as above due to negligible time-averaged vertical velocity component, and  $\varepsilon_t$  is the turbulent diffusivity. At the centerline ( $r = r_c$ ) of the meandering rivers,  $\varphi = 1$ ,  $U = \bar{U}$ , and  $H = h$ . Using  $r_c^{-1} = r_{c0}^{-1} \cos(k_{wb}s)$ , Eq. (9.19) at the centerline becomes

$$\bar{U} \frac{\partial \Omega_s}{\partial s} - \frac{2 \cos(k_{wb}s)}{r_{c0}} \bar{U} \frac{\partial \bar{U}}{\partial z} = \varepsilon_t \frac{\partial^2 \Omega_s}{\partial z^2} \quad (9.20)$$

Substituting Eqs. (9.17) and (9.18) into Eq. (9.20) and then equating the coefficients of  $\sin(k_{wb}s)$  and  $\cos(k_{wb}s)$  to obtain two equations, the  $\chi$  and  $\sigma_L$  are solved as

$$\chi = 2 \frac{dG}{d\hat{\eta}} \left( k_{wb} h \frac{\bar{U}}{\bar{u}_*} \cdot \frac{d\varphi_0}{d\hat{\eta}} \sin \sigma_L - \frac{\varepsilon_t}{\bar{u}_* h} \cdot \frac{d^3 \varphi_0}{d\hat{\eta}^3} \cos \sigma_L \right)^{-1} \quad (9.21a)$$

$$\sigma_L = \arctan \left[ k_{wb} h \frac{d\varphi_0}{d\hat{\eta}} \left( \frac{\varepsilon_t}{\bar{u}_* h} \cdot \frac{\bar{u}_*}{\bar{U}} \cdot \frac{d^3 \varphi_0}{d\hat{\eta}^3} \right)^{-1} \right] \quad (9.21b)$$

Ikeda et al. (1985) proposed  $\varepsilon_t/(\bar{u}_* h) = 0.1$  for the flow in sinuous rivers. Then,  $\chi$  and  $\sigma_L$  take the forms

$$\chi = \left[ k_{wb} h \left( \frac{1.11}{\lambda_f^{0.5}} - 1.42 \right) \sin \sigma_L + \cos \sigma_L \right]^{-1} \quad (9.22a)$$

$$\sigma_L = \arctan \left[ k_{wb} h \left( \frac{1.11}{\lambda_f^{0.5}} - 1.42 \right) \right] \quad (9.22b)$$

Note that  $k_{wb}h = 1.5\lambda_f$ , as already stated.

The estimation of  $\bar{u}(z)$  is possible from Eq. (9.17) using Eqs. (9.11), (9.14) and (9.15); and the time-averaged transverse velocity component  $\bar{v}(z)$  can be calculated from the decomposition relationship  $\bar{v} = V' + v''$ , where  $V'$  is given by Eq. (9.16) and  $v''$  can be obtained from Eq. (9.18) using Eqs. (9.22a, b).

### 9.3.1.2 Bed Deformation

In equilibrium state, the continuity equation of sediment transport resulting in a change of bed level is given and then its integral form is obtained as

$$\begin{aligned} \frac{r_c}{r} \cdot \frac{\partial q_{ts}}{\partial s} + \frac{1}{r} \cdot \frac{\partial (rq_{tn})}{\partial n} = 0 \quad \wedge \quad q_{ts} = q_{bs} + q_{ss} \quad \vee \quad q_{tn} = q_{bn} + q_{sn} \\ \Rightarrow q_{tn} = -\frac{r_c}{r} \int \frac{\partial q_{ts}}{\partial s} dn \end{aligned} \quad (9.23)$$

where  $q_{ts}$  and  $q_{tn}$  are the volumetric total-load transport rate in  $s$ - and  $r$ -direction, respectively,  $q_{bs}$  and  $q_{bn}$  are the volumetric bed-load transport rate in  $s$ - and  $r$ -direction, respectively, and  $q_{ss}$  and  $q_{sn}$  are the volumetric suspended-load transport rate in  $s$ - and  $r$ -direction, respectively.

Ikeda and Nishimura used Parker's (1979) formula, (Eq. 5.24), to estimate  $q_{bs}$ . Equation (5.24) is rearranged as

$$q_{bs} = 11.2(\Delta g d_{50}^3)^{0.5} \frac{(\Theta - 0.03)^{4.5}}{\Theta^3} \quad (9.24)$$

where  $\Theta$  is the Shields parameter, which is  $u_*^2/(\Delta g d_{50})$  for a horizontal bed of a straight river. Here,  $u_*$  is the local shear velocity. Due to helicoidally curvilinear flow in meandering rivers,  $\Theta$  is corrected as

$$\Theta = \varphi^2 \left( \frac{U}{\bar{U}} \right)^2 \frac{\bar{u}_*^2}{\Delta g d_{50}} \quad (9.25)$$

Parker (1984) gave

$$\frac{q_{bn}}{q_{bs}} = \tan \beta + \frac{1 + \eta_R \mu}{\zeta_s \mu} \left( \frac{\Theta_c}{\Theta} \right)^{0.5} \tan \alpha \quad \wedge \quad \alpha = \arctan \frac{\partial \eta}{\partial n}$$

where  $\beta$  is the angle made by the near-bed limiting streamline with  $s$ -direction, that is,  $\arctan(\bar{v}_d/\bar{u}_d)$ ,  $\bar{v}_d$  is the near-bed time-averaged transverse velocity,  $\bar{u}_d$  is the near-bed time-averaged streamwise velocity,  $\Theta_c$  is the threshold Shields parameter, and  $\alpha$  is the angle made by the transverse bed slope with horizontal. For sand-beds, Kikkawa et al. (1976) approximated  $\mu$ ,  $\eta_R$ , and  $\zeta_s$  as 0.43, 0.85 and 0.59, respectively; and the above equation becomes

$$\frac{q_{bn}}{q_{bs}} = \tan \beta + 5.38 \left( \frac{\Theta_c}{\Theta} \right)^{0.5} \frac{\partial \eta}{\partial n} \quad (9.26)$$

Ikeda and Nishimura obtained  $\bar{u}_d$  from the logarithmic law of velocity distribution for hydraulically rough flow applied to the roughness height level  $k_s$  as

$$\begin{aligned} \bar{u}_d &= u_* \left( 8.5 + \frac{1}{\kappa} \ln \frac{z+H}{k_s} \right) \Big|_{z=-H+k_s} = 8.5 u_* \quad \wedge \quad u_* = \varphi \frac{U}{U} \bar{u}_* \\ \Rightarrow \bar{u}_d &= 8.5 \varphi \frac{U}{U} \bar{u}_* \end{aligned} \quad (9.27)$$

They obtained  $\bar{v}_d$  from the relationship  $\bar{v} = V' + v''$ , where  $v''(\hat{\eta} = 0)$  at the bed is obtained from Eq. (9.18). Then,  $\tan \beta$  is given by

$$\tan \beta = \left[ \frac{V'}{U} + \varphi^2 \left( \frac{U}{U} \right)^2 \frac{H}{\kappa r} \chi \varphi_0(0) \frac{r_c}{r_{c0}} \cos(k_{wb}s - \sigma_L) \right] \left[ 8.5 \varphi \left( \frac{U}{U} \right) \lambda_f^{0.5} \right]^{-1} \quad (9.28)$$

where  $\varphi_0(0) = -4.167 + 2.64 \lambda_f^{0.5} \kappa^{-1}$ .

The suspended-load transport rate  $q_{ss}$  in  $s$ -direction and time-averaged concentration distribution  $C(z)$  are given by

$$q_{ss} = \int_{-H}^0 C \bar{u} dz \quad (9.29a)$$

$$C = C_a \exp \left[ -\frac{w_s}{\varepsilon_s} (z + H) \right] \quad (9.29b)$$

where  $C_a$  is the near-bed concentration,  $w_s$  is the terminal fall velocity of sediment, and  $\varepsilon_s$  is the sediment diffusivity. Above equations are the modified forms of Eqs. (6.1a) and (6.20) due to change of position of the origin of  $z$ -axis. The sediment diffusivity  $\varepsilon_s$  can be assumed as follows (Vanoni 1975):



$$\varepsilon_s = 0.077u_*H \quad (9.30)$$

Further, Ikeda and Nishimura (1985) gave  $C_a$  in empirical form as

$$C_a(u_* \leq 88.3w_s) = 2.31 \times 10^{-4} \left( \frac{u_*}{w_s} \right)^{1.6}, \quad C_a(u_* > 88.3w_s) = 0.3 \quad (9.31)$$

Inserting Eqs. (9.17) and (9.29b) into Eq. (9.29a) yields

$$\frac{q_{ss}}{UH} = \varphi \frac{U}{U} \Phi_{ss} \quad (9.32)$$

where

$$\begin{aligned} \Phi_{ss} = & C_a \{ [\psi_1 - \psi_2 \exp(\varpi^{-1})] \varpi + [\psi_3 - \psi_4 \exp(\varpi^{-1})] \varpi^2 \\ & + [\psi_5 - \psi_6 \exp(-\varpi^{-1})] \varpi^3 + \psi_7 [1 - \exp(-\varpi^{-1})] \varpi^4 \}, \\ \varpi = & \varepsilon_s / (w_s H) = 0.077u_* / w_s = 0.077\varphi U \bar{u}_* / (\bar{U} w_s), \quad \psi_1 = 1 - 5.798\lambda_f^{0.5}, \\ \psi_2 = & 1 + 2.678\lambda_f^{0.5}, \quad \psi_3 = 26.6\lambda_f^{0.5}, \quad \psi_4 = 6.95\lambda_f^{0.5}, \quad \psi_5 = -69.45\lambda_f^{0.5}, \\ \psi_6 = & 30.15\lambda_f^{0.5}, \text{ and } \psi_7 = 99.6\lambda_f^{0.5}. \end{aligned}$$

The suspended-load transport rate  $q_{sn}$  in  $n$ -direction is given by

$$q_{sn} = \int_{-H}^0 C \bar{v} dz \quad (9.33)$$

Inserting expressions for  $\bar{v} (= V' + v'')$  and Eq. (9.29b) into Eq. (9.33) yields

$$\frac{q_{sn}}{UH} = \frac{V'}{\bar{U}} \Phi_{sn1} - \varphi^2 \left( \frac{U}{\bar{U}} \right)^2 \frac{H}{\kappa r} \chi \frac{r_c}{r_{c0}} \cos(k_{wb}s - \sigma_L) \Phi_{sn2} \quad (9.34)$$

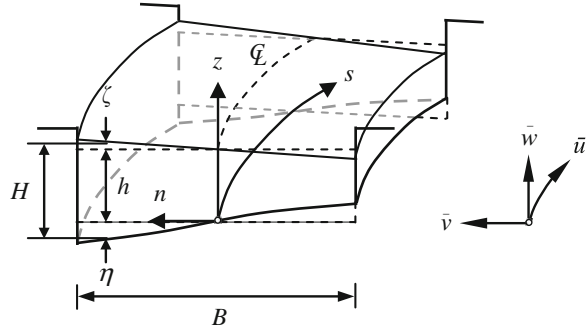
where  $\Phi_{sn1} = C_a [1 - \exp(-\varpi^{-1})] \varpi$ ,  $\Phi_{sn2} = C_a \{ [\xi_1 \exp(-\varpi^{-1}) - \xi_2] \varpi + [\xi_3 \exp(-\varpi^{-1}) - \xi_4] \varpi^2 + [\xi_5 \exp(-\varpi^{-1}) - \xi_6] \varpi^3 - 72.34 [\exp(-\varpi^{-1}) - 1] \varpi^4 \}$ ,  $\xi_1 = 3.26 - 2.58\lambda_f^{0.5}$ ,  $\xi_2 = -4.29 + 7.005\lambda_f^{0.5}$ ,  $\xi_3 = -1.57 + 3.69\lambda_f^{0.5}$ ,  $\xi_4 = 4.61 - 22.86\lambda_f^{0.5}$ ,  $\xi_5 = -42.36 + 26.55\lambda_f^{0.5}$ , and  $\xi_6 = 15 + 13.28\lambda_f^{0.5}$ .

Equation of bed-level variation can be obtained by substituting Eq. (9.26) into Eq. (9.23) as

$$\frac{\partial \eta}{\partial n} = -0.186 \left( \frac{\Theta}{\Theta_c} \right)^{0.5} \frac{1}{q_{bs}} \left[ \frac{r_c}{r} \int \frac{\partial}{\partial s} (q_{bs} + q_{ss}) dn + q_{sn} + q_{bs} \tan \beta \right] \quad (9.35)$$

The bed- and suspended-load transport rates,  $q_{bs}$ ,  $q_{bn}$ ,  $q_{ss}$ , and  $q_{sn}$ , are obtained from Eqs. (9.24), (9.26), (9.32) and (9.34), respectively. The partial derivative

**Fig. 9.13** Definition sketch showing cross-section of a sinusoidal river



$\partial q_{bs}/\partial s$  can be obtained from Eq. (9.24) by using Eqs. (9.11), (9.14) and (9.25). Further,  $\partial q_{ss}/\partial s$  can be obtained from Eq. (9.32) in terms of  $H$  and  $u_*$ . Using the relationship given by Ikeda et al. (1981), that is,  $\zeta = Fr^2 hn/r_c$ , and Eq. (9.13),  $H$  is expressed as

$$H = h \left[ Fr^2 \frac{n}{r_c} + \left( \frac{r}{r_c} \right)^\vartheta \right] \quad (9.36)$$

Thus, the term  $\partial(q_{bs} + q_{ss})/\partial s$  in Eq. (9.35) can take the form

$$\begin{aligned} & \frac{1}{U} \cdot \frac{1}{k_{wb}} \cdot \frac{\partial}{\partial s} (q_{bs} + q_{ss}) \\ &= \varphi \frac{n}{r_{c0}} \left\{ \Psi_{bs} + \left[ Fr^2 \frac{n}{r_c} + \left( \frac{r}{r_c} \right)^\vartheta \right] (\Phi_{ss} + \Psi_{ss}) \right\} \\ & \times [a \cos(k_{wb}s) - b \sin(k_{wb}s)] - \varphi \frac{U}{U} \cdot \frac{n}{r_{c0}} \left[ Fr^2 + \vartheta \left( \frac{r}{r_c} \right)^{\vartheta-1} \right] \Phi_{ss} \sin(k_{wb}s) \end{aligned} \quad (9.37)$$

where

$$\Psi_{bs} = 33.6 \frac{(\Delta g d_{50}^3)^{0.5}}{U h} \varphi \frac{U}{U} \cdot \frac{\bar{u}_*^2}{\Delta g d_{50}} \cdot \frac{(\Theta + 0.06)(\Theta - 0.03)^{3.5}}{\Theta^4},$$

$\Psi_{ss} = C_a \{-\gamma_1 \exp(-\varpi^{-1}) + [\gamma_2 - \gamma_3 \exp(-\varpi^{-1})] \varpi + [\gamma_4 - \gamma_5 \exp(-\varpi^{-1})] \varpi^2 + [\gamma_6 - \gamma_7 \exp(-\varpi^{-1})] \varpi^3 + \gamma_8 [1 - \exp(-\varpi^{-1})] \varpi^4\}$ ,  $\gamma_1 = 26.6 \lambda_f^{0.5}$ ,  $\gamma_2 = 2.6 - 15.07 \lambda_f^{0.5}$ ,  $\gamma_3 = 2.6 + 13.91 \lambda_f^{0.5}$ ,  $\gamma_4 = 95.76 \lambda_f^{0.5}$ ,  $\gamma_5 = 55.17 \lambda_f^{0.5}$ ,  $\gamma_6 = -319.5 \lambda_f^{0.5}$ ,  $\gamma_7 = 238.3 \lambda_f^{0.5}$ , and  $\gamma_8 = 557.8 \lambda_f^{0.5}$ . Then, the integration in Eq. (9.35) can be performed with the determination of integral constant from the condition that the average variation of bed level across the cross-section is zero, that is

$$\int_{-0.5B}^{0.5B} \eta dn = 0$$

### 9.3.2 Odgaard's Model

#### 9.3.2.1 Flow Field and Bed Topography

Odgaard (1989) considered orthogonal curvilinear coordinates  $(s, n, z)$  to represent time-averaged velocity components  $(\bar{u}, \bar{v}, \bar{w})$  and bed variations, as shown in Fig. 9.13. The plan view of a sinusoidal river is same as shown in Fig. 9.12a. In meandering rivers, the prevailing conditions are the flow depth to be smaller than the flow width ( $H \ll B$ ) and the radius of curvature to be generally larger than the width ( $r_c > B$ ). Under these conditions, all the terms containing  $\bar{w}$  can be dropped out in momentum and continuity equations as  $\bar{w} \rightarrow 0$ . This approximation makes the problem a two-dimensional. According to Rozovskii (1957), the two-dimensional momentum equations of flow can be written as

$$\bar{u} \frac{\partial \bar{u}}{\partial s} + \bar{v} \frac{\partial \bar{u}}{\partial n} + \frac{\bar{u}\bar{v}}{r} = \frac{1}{\rho} \left( -\frac{\partial \bar{p}}{\partial s} + \frac{\partial \tau_s}{\partial z} \right) \quad (9.38a)$$

$$\bar{u} \frac{\partial \bar{v}}{\partial s} + \bar{v} \frac{\partial \bar{v}}{\partial n} - \frac{\bar{u}^2}{r} = \frac{1}{\rho} \left( -\frac{\partial \bar{p}}{\partial n} + \frac{\partial \tau_n}{\partial z} \right) \quad (9.38b)$$

where  $r$  is the local radius of curvature,  $\bar{p}$  is the time-averaged hydrostatic pressure, and  $\tau_s$  and  $\tau_n$  are the shear stresses in  $s$ - and  $n$ -direction, respectively. The continuity equations of flow and sediment transport are

$$\frac{\partial \bar{u}}{\partial s} + \frac{1}{r} \cdot \frac{\partial (\bar{v}r)}{\partial n} = 0 \quad (9.39a)$$

$$\frac{\partial q_{bs}}{\partial s} + \frac{1}{r} \cdot \frac{\partial (q_{bn}r)}{\partial n} = 0 \quad (9.39b)$$

where  $q_{bs}$  and  $q_{bn}$  are the bed-load transport in  $s$ - and  $n$ -direction, respectively.

The integration (with respect to depth) of the pressure containing terms in Eqs. (9.38a, b) can be expressed in terms of the free-surface slopes ( $S_s$  and  $S_n$ ) as  $-gS_s$  in  $s$ -direction and  $-gS_n$  in  $n$ -direction. Here,  $g$  is the acceleration due to gravity. Thus, the depth-averaged momentum and continuity equations become

$$U \frac{\partial U}{\partial s} + V \frac{\partial U}{\partial n} + \frac{UV}{r} = gS_s - \frac{\tau_{0s}}{\rho H} \quad (9.40a)$$

$$U \frac{\partial V}{\partial s} + V \frac{\partial V}{\partial n} - \frac{U^2}{r} = gS_n - \frac{\tau_{0n}}{\rho H} \quad (9.40b)$$

and

$$\frac{\partial(UH)}{\partial s} + \frac{1}{r} \cdot \frac{\partial(VHr)}{\partial n} = 0 \quad (9.41)$$

where  $U$  and  $V$  are the depth-averaged velocities in  $s$ - and  $n$ -direction, respectively, and  $\tau_{0s}$  and  $\tau_{0n}$  are the bed shear stresses in  $s$ - and  $n$ -direction, respectively. In the above, the approximate relationships are used as  $\bar{u}\bar{v} \approx UV$  and  $\bar{u}\bar{u} \approx U^2$ , which are based on the field and laboratory experimental data (Dietrich and Smith 1983; Bergs 1989).

The  $\bar{u}$  distribution is represented by a power law as

$$\frac{\bar{u}}{U} = \frac{1+m}{m} \left( \frac{z}{H} \right)^{1/m} \quad \wedge \quad m = \kappa \frac{U}{u_*} = \kappa \left( \frac{8}{\lambda_D} \right)^{0.5} = \kappa \frac{C_R}{g^{0.5}} \quad \vee \quad u_* = \left( \frac{\tau_{0s}}{\rho} \right)^{0.5} \quad (9.42)$$

where  $m$  is an exponent indicating resistance to flow,  $\lambda_D$  is the Darcy–Weisbach friction factor, and  $C_R$  is the Chézy coefficient. Above relationship for  $m$  was given by Zimmermann and Kennedy (1978). In bankfull conditions, the  $m$  is  $3 \leq m \leq 5$ .

On the other hand, the  $\bar{v}$  distribution is represented as an addition of  $V$  and centrifugally induced transverse velocity component  $v''(z)$  of the secondary current, which is approximated by a linear law as  $2v_0''[(z/H)-0.5]$ , where  $v_0'' = v''(z = h + \zeta)$  (Rozovskii 1957; Kikkawa et al. 1976). Thus,

$$\bar{v} = V + v'' = V + 2v_0'' \left( \frac{z}{H} - \frac{1}{2} \right) \quad (9.43)$$

Subtracting Eq. (9.40b) from Eq. (9.38b) at  $z = h + \zeta$  yields

$$\bar{u}_0 \frac{\partial \bar{v}_0}{\partial s} - U \frac{\partial V}{\partial s} + \bar{v}_0 \frac{\partial \bar{v}_0}{\partial n} - V \frac{\partial V}{\partial n} = \frac{\bar{u}_0^2 - U^2}{r} + \frac{\tau_{0n}}{\rho H} + \frac{1}{\rho} \cdot \frac{\partial \tau_n}{\partial z} \Big|_{z=h+\zeta} \quad (9.44)$$

where  $\bar{u}_0 = \bar{u}(z = h + \zeta)$  and  $\bar{v}_0 = \bar{v}(z = h + \zeta)$ . The partial derivative in the last term of the right-hand side of Eq. (9.44) can be determined as

$$\frac{\partial \tau_n}{\partial z} = \frac{\partial}{\partial z} \left( \varepsilon_t \frac{\partial \bar{v}}{\partial z} \right)$$

Then, by solving  $\varepsilon_t$  from the power law and  $\tau_s = \tau_{0s}[1 - (z/H)]$  and assuming an isotropic  $\varepsilon_t$  with  $\bar{v}$  given by Eq. (9.43), the above partial derivative at free surface is obtained as

$$\left. \frac{\partial \tau_n}{\partial z} \right|_{z=h+\zeta} = -\frac{m}{1+m} \cdot \frac{2\rho\kappa v_0'' u_*}{H} \quad (9.45)$$

The ratio of  $\tau_{0n}$  to  $\tau_{0s}$  is obtained from the deflection of the near-bed limiting streamline from  $s$ -axis, that is,  $\tan\beta = \bar{v}_d/\bar{u}_d$ . Then,

$$\frac{\tau_{0n}}{\tau_{0s}} = \frac{\bar{v}_d}{\bar{u}_d} = \frac{V - v_0''}{U} \quad (9.46)$$

Note that the expression for  $m$  in Eq. (9.42) leads to

$$\tau_{0s} = \rho\kappa^2 \frac{1}{m^2} U^2 \quad (9.47)$$

Substituting Eqs. (9.42), (9.43) and (9.47) into Eq. (9.40a) yields

$$\frac{1}{2} \cdot \frac{\partial U^2}{\partial s} + \frac{\kappa^2}{m^2 H} U^2 = gS_s - V \left( \frac{\partial U}{\partial n} + \frac{U}{r} \right) \quad (9.48)$$

Substituting Eqs. (9.42), (9.43), (9.45) and (9.46) into Eq. (9.44) yields

$$\begin{aligned} \frac{\partial V}{\partial s} + (1+m) \frac{\partial v_0''}{\partial s} + \frac{m}{U} \cdot \frac{\partial (v_0'' V)}{\partial n} + \frac{m}{2U} \cdot \frac{\partial (v_0'' v_0'')}{\partial n} \\ = \frac{1+2m}{m} \cdot \frac{U}{r} + \frac{\kappa^2}{mH} V - \frac{\kappa^2}{mH} \left( 1 + \frac{2m^2}{1+m} \right) v_0'' \end{aligned} \quad (9.49)$$

Thus, the above mathematical analysis produces Eqs. (9.39a, b), (9.48) and (9.49) as governing equations for solving  $V$ ,  $H$ ,  $U$ , and  $v_0''$ , respectively.

From field and laboratory results, Odgaard argued that the variables  $\bar{u}$  and  $H$  are essentially constant along the centerline, but vary somewhat linearly in transverse direction. Hence, they are linearized with respect to their centerline values:

$$\frac{U}{U_c} = 1 + \frac{n}{h} \tilde{U}_{cn} \quad \wedge \quad \tilde{U}_{cn} = \left[ h \frac{\partial}{\partial n} \left( \frac{U}{U_c} \right) \right]_c \quad (9.50a)$$

$$\frac{H}{h} = 1 + \frac{n}{h} S_{cn} \quad \wedge \quad S_{cn} = \left. \frac{\partial H}{\partial n} \right|_c \quad (9.50b)$$

where  $U_c$  and  $h$  are the depth-averaged velocity and flow depth at the centerline, respectively,  $\tilde{U}_{cn}$  is the nondimensional transverse velocity gradient at the centerline, and  $S_{cn}$  is the transverse gradient of the bed at the centerline. In the above,



subscript “c” refers to the centerline value. From Eq. (9.41),  $V_c$  is obtained as an integral equation and then solved using Eqs. (9.50a, b) and  $r = r_c + n$ . Thus,

$$V_c = \frac{1}{hr_c} \cdot \frac{d}{ds} \int_0^{0.5B} rUHdn \Rightarrow V_c = \frac{\alpha_n}{8} U_c \frac{B^2}{h} \cdot \frac{d}{ds} (S_{cn} + \tilde{U}_{cn}) \quad (9.51)$$

where  $\alpha_n$  is the transverse flux correction factor having an average value of 0.4.

Odgaard assumed  $q_{bs} = [q_{bs}]_c (U/U_c)^M$ , where  $[q_{bs}]_c$  is the bed-load transport rate in  $s$ -direction at the centerline and  $M$  is an exponent varying from 2 to 4 (Simons and Sentürk 1977). Then, integration of Eq. (9.39b) yields

$$[q_{bn}]_c = \frac{1}{r_c} \cdot \frac{d}{ds} \int_0^{0.5B} q_{bs} r dn \Rightarrow [q_{bn}]_c = [q_{bs}]_c \frac{\beta_n}{8} \cdot \frac{B^2}{h} M \frac{d\tilde{U}_{cn}}{ds} \quad (9.52)$$

where  $[q_{bn}]_c$  is the bed-load transport rate in  $n$ -direction at the centerline and  $\beta_n$  is the transverse sediment flux correction factor have an order of magnitude same as that of  $\alpha_n$ .

Using Eqs. (9.26), (9.46) and (9.47), Eq. (9.52) yields

$$\frac{5.38}{\kappa} m (\Delta g d_{50})^{0.5} \Theta^{0.5} S_{cn} = \frac{\alpha_n}{8} \cdot \frac{B^2}{h} U_c M \frac{d\tilde{U}_{cn}}{ds} + [v_0]_c - V_c \quad (9.53)$$

Substituting Eqs. (9.50a, b), (9.51) and (9.53) into Eqs. (9.48) and (9.49) and neglecting higher order terms, the resulting linear equations are

$$\frac{d\tilde{U}_{cn}}{d\hat{s}} + a_1 \tilde{U}_{cn} = \frac{1}{2} a_1 S_{cn} \quad \wedge \quad \hat{s} = \frac{s}{B} \quad (9.54a)$$

$$\frac{d^2 S_{cn}}{d\hat{s}^2} + a_2 \frac{d^2 \tilde{U}_{cn}}{d\hat{s}^2} + a_3 \frac{dS_{cn}}{d\hat{s}} + a_4 \frac{d\tilde{U}_{cn}}{d\hat{s}} + a_5 S_{cn} = a_6 \quad (9.54b)$$

where

$$\begin{aligned} a_1 &= \frac{2\kappa^2}{m^2} \cdot \frac{B}{h}, \quad a_2 = 1 - \frac{1+m}{2+m} M, \quad a_3 = 43 \frac{\Theta^{0.5}}{\alpha_n \kappa F_d} \cdot \frac{m(1+m)}{2+m} \cdot \frac{h}{B} \\ &+ \frac{2\kappa^2 m}{(1+m)(2+m)} \cdot \frac{B}{h}, \quad a_4 = \frac{2\kappa^2 m}{(1+m)(2+m)} \left[ 1 - M \left( 1 + \frac{1}{2m} + \frac{1}{2m^2} \right) \right] \frac{B}{h}, \\ a_5 &= 43 \frac{\kappa \Theta^{0.5}}{\alpha_n (2+m) F_d} \left( 1 + \frac{2m^2}{1+m} \right), \quad a_6 = \frac{8}{\alpha_n} \cdot \frac{1+2m}{m(2+m)} \cdot \frac{h}{r_c} \end{aligned}$$

where  $F_d$  is the densimetric Froude number  $[= U_c / (\Delta g d_{50})^{0.5}]$ . Further, using Eq. (9.54a), Eq. (9.54b) is rearranged as

$$\frac{d^3 \tilde{U}_{cn}}{d\hat{s}^3} + b_1 \frac{d^2 \tilde{U}_{cn}}{d\hat{s}^2} + b_2 \frac{d\tilde{U}_{cn}}{d\hat{s}} + b_3 \tilde{U}_{cn} = b_4 \quad (9.55)$$

where  $b_1 = a_1 + 0.5a_1a_2 + a_3$ ,  $b_2 = a_1a_3 + 0.5a_1a_4 + a_5$ ,  $b_3 = a_1a_5$ , and  $b_4 = 0.5a_1a_6$ . Equation (9.55) can be solved for  $\tilde{U}_{cn}$  for the given boundary conditions, and then,  $S_{cn}$  can be determined from Eq. (9.54a).

Note that in fully developed flow in a channel bend, the terms  $d(\cdot)/d\hat{s} = 0$ , and Eqs. (9.54a, b) reduce to

$$\frac{U}{U_c} = \left(\frac{H}{h}\right)^{0.5}, \quad S_{cn0} = \frac{GF_{dc}h}{r_c} \quad \wedge \quad G = \frac{(1+m)(1+2m)}{5.38\kappa\Theta^{0.5}m(1+m+2m^2)}$$

where  $S_{cn0}$  is the fully developed value of  $S_{cn}$  and  $F_{dc}$  is the  $F_d$  at the centerline.

An approximate solution of Eqs. (9.54a, b) can be obtained assuming  $d^2\tilde{U}_{cn}/d^2\hat{s}$  to be negligible. Then, Eqs. (9.54a, b) produce

$$\frac{d^2 S_{cn}}{d\hat{s}^2} + \left(a_3 + \frac{a_4}{2}\right) \frac{dS_{cn}}{d\hat{s}} + a_5 S_{cn} = a_6 \quad (9.56)$$

At the starting section of the bend (that is  $\hat{s} = 0$ ), both  $S_{cn}$  and  $dS_{cn}/d\hat{s}$  vanish; and the solution of Eq. (9.56) is

$$S_{cn} = S_{cn0} \left\{ 1 - \left[ 1 + \left( \frac{a_0}{2\phi_0} \right)^2 \right]^{0.5} \cos(\phi_0\hat{s} - \psi_0) \exp\left(-\frac{a_0\hat{s}}{2}\right) \right\} \quad (9.57)$$

where  $\phi_0 = 0.5(4a_5 - a_0^2)^{0.5}$ ,  $a_0 = a_3 + 0.5a_4$ , and  $\psi_0 = \arctan(0.5a_0/\phi_0)$ .

### 9.3.2.2 Stability of Meandering Rivers

In stability analysis, Odgaard (1989) introduced a small perturbation in the form of a traveling sinusoidal wave to the system of governing equations of a river flow coupled with the sediment transport. Then, their effect on river planform is determined by evaluating the growth rate of perturbation. The perturbation due to a traveling sinusoidal wave is introduced as river displacement  $\xi(x, t)$  given by

$$\xi(x, t) = a_{mc}(t) \sin[k_{wb}(x - ct)] \quad (9.58)$$

where  $x$  is the coordinate distance along the unperturbed river axis or the valley slope (Fig. 9.12a),  $k_{wb}$  is the wave number ( $= 2\pi/\lambda_m$ ),  $a_{mc}$  is the amplitude,  $\lambda_m$  is the meandering wavelength,  $c$  is the celerity of sinusoidal wave, and  $t$  is the time.

Approximating local radius of curvature as  $r_c^{-1} = -d^2\xi/dx^2$  and using Eq. (9.58), Eq. (9.55) is solved for  $\tilde{U}_{cn}$  as

$$\tilde{U}_{cn} = \frac{Bk_{wb}^2 a_{mc}}{(e_1^2 + e_2^2)^{0.5}} N \sin[k_{wb}(x - ct) - \gamma_0] \quad \wedge \quad \gamma_0 = \arctan\left(\frac{e_2}{e_1}\right) \quad (9.59)$$

where  $e_1 = b_3 - 2b_1 B^2 k_{wb}^2$ ,  $e_2 = b_2 B k_{wb} - k_{wb}^3 B^3$ , and

$$N = \frac{8\kappa^2}{\alpha_n} \cdot \frac{1 + 2m}{m^3(2 + m)}.$$

Substituting Eq. (9.59) into Eq. (9.54a) yields

$$S_{cn} = \frac{2Bk_{wb}^2 a_{mc}}{(e_1^2 + e_2^2)^{0.5}} N \left[ 1 + \left( \frac{Bk_{wb}}{a_1} \right)^2 \right]^{0.5} \sin[k_{wb}(x - ct) - \beta_0] \quad (9.60)$$

where  $\beta_0 = \gamma_0 - \arctan(Bk_{wb}/a_1)$ .

Odgaard assumed that the rate of bank retreat  $\xi_b$  is linearly proportional to the change of bed level at the bank:

$$\xi_b = EU_c \left( \frac{H_{bank}}{h} - 1 \right) \quad (9.61)$$

where  $E$  is the erosion parameter and  $H_{bank}$  is the near-bank value of  $H$ . Due to small curvature of the river,  $\xi_b \approx \partial \xi / \partial t$ . The closure of the analysis is achieved by substituting Eq. (9.58) into left-hand side of Eq. (9.61) and Eqs. (9.59) and (9.60) into right-hand side of Eq. (9.61). Performing required simplifications, the equations of growth rate of amplitude  $\partial a_{mc} / \partial t$  and celerity  $c$  are obtained as follows:

$$\frac{1}{a_{mc}} \cdot \frac{\partial a_{mc}}{\partial t} = \frac{2EU_c}{B} KBk_{wb} \left[ 1 + \left( \frac{Bk_{wb}}{a_1} \right)^2 \right]^{0.5} \cos \beta_0 \quad \wedge \quad K = \frac{NB}{2h} \cdot \frac{Bk_{wb}}{(e_1^2 + e_2^2)^{0.5}} \quad (9.62a)$$

$$c = 2EU_c K \left[ 1 + \left( \frac{Bk_{wb}}{a_1} \right)^2 \right]^{0.5} \sin \beta_0 \quad (9.62b)$$

Note that the wave number  $k_{wb}$  corresponding to maximum amplitude growth, called *dominant wave number*, can be determined from the following condition:

$$\frac{\partial^2 a_{mc}}{\partial t \partial k_{wb}} = 0$$

## 9.4 Braided Rivers

Braided rivers are quite dynamic with strong fluvial activities (interactions between streambed morphology, flow, and sediment transport) to follow rapidly change in subdivided stream forms. The bars and islands characterize braiding by dividing streams by their sides. While bars are relatively unstable having complex features, islands are rather stable with well-defined shapes. Bars are modified by the processes of erosion and deposition and evolve over a short period of time. During high flow stages, major changes take place due to rapid rates of stream migration facilitated by high stream power and unstable banks. There can also be extensive changes in stream position as subdivided streams are abandoned or earlier abandoned streams are reactivated. However, even in a braided reach, a single dominant stream, in some cases, can be distinguishable. Planform of braided rivers can change radically with the change in discharge. For instance, Bristow and Best (1993) argued that the discharge fluctuations are a prerequisite for braiding especially in sand-bed rivers. Rivers may act as a single stream during bankfull conditions and exhibit characteristic braided pattern at lower stages. Therefore, the number of bars to be emerged may vary with flow stages; as such, complex sequence of erosion and deposition may occur with the variation of flow stages. Nevertheless, at both low and high stages, some of the rivers show braided pattern where some of the islands are in general permanent. Southard et al. (1984) reported that the process of bar growth and streambed erosion occurs almost simultaneously, and the majority of the emerged bars are the result of complex events of erosion and deposition. Robert (2003) gave a good overview on braided rivers.

Lane (1957) studied planforms of many braided rivers and their history. He came out with a conclusion that the braiding can be caused by (1) overloading and (2) steep slopes. *Overloading* refers to when the sediment discharge (inflow transport rate) exceeds the sediment capacity (outflow transport rate) of a river depositing sediment load (aggradations) throughout the reach. As a consequence, the river carrying most of the sediment load gradually changes its morphology as the excess sediment load settles progressively in the downstream direction. Besides, the fining of bed sediment size takes place in the downstream direction and is usually accompanied by a downstream reduction in bed slope. The deposition of sediment in an aggrading river makes it out of bankfull conditions. The river tends to widen and becomes shallow with an appearance of bars subjected to changes in morphology. At low stages, a series of small streams divide and rejoin through the exposed bars in more or less regular and repeatable processes. These streams are braided as the bed slope enhances with aggradations. On the other hand, *steep slope* that induces greater stream power for the given discharge results in a wide shallow river in which bars and islands are readily developed. Stream subdivision is continued until there is inadequate stream power to erode the banks (Leopold and Wolman 1957). A distinction is often made between bars and islands, although they have the same origin and may share similar morphological characteristics. While bars are only developed at low stages being unvegetated, but

often submerged in bankfull conditions, islands are more stable and may be vegetated, but emerge even in bankfull conditions.

Carson and Griffiths (1987) recognized three types of braided rivers: unstable multiple stream, stable multiple stream, and multi-thalweg. In *unstable multiple-stream pattern*, streams are separated by the bars and can be rapidly diverted from one stream to another depending on sediment deposition. *Stable multiple-stream pattern* consists of relatively stable streams even during high flow stages with subdivided streams separated by stable vegetated islands. On the other hand, *multi-thalweg* pattern is characterized by braids being separated by submerged bars during high flow stages.

### 9.4.1 Mechanism of Braid Formation

Complex mechanisms are involved in inception and development of braided planforms, depending on the stream flow characteristics and both erosional and depositional processes. Ashmore (1991) identified four types of mechanisms of braid formation: middle bar accretion, transverse bar conversion, chute cutoff, and multiple bar dissection. A summary of various mechanisms put forward by different investigators is presented below:

Leopold and Wolman (1957) were the first to study the mechanism of inception and development of braided planforms through laboratory experiments. They identified that the development of braided planforms by *middle bar accretion* takes place through a sequence of events that comprise of deposition in mid-river and erosion of banks. The characteristic shape of middle bars (also called *linguoid bars*) is rhombic or lobate in plan view and elongated in streamwise direction. In an unbraided river reach, localized flow converges to a high velocity at the upstream end of the narrower flanking river reach leading to an excessive erosion. It forms a sheet of bed-load sediment (that includes coarser to finer size fractions) that is transported along the riverbed. In transporting the bed load, a small submerged gravel bar where the flow becomes locally incompetent to transport the coarsest particles, called *lag deposits*, is formed. The upstream of the bar margin is made up by the coarse fraction of bed-load sediment that is transported along the middle portion of the river. Finer particles are in general transported over the bar, while a fraction of finer particles are deposited on the bar and/or trapped behind the coarser particles, leading to the enlargement of the emerging bar in all dimensions (vertical, streamwise, and transverse directions). Once the bar becomes sufficiently large, it starts affecting the divided streams along its sides by increase in the flow velocity or in turn, the stream power, which begins to attack the banks and widens the river by bank erosion. The bar gradually gets stabilized due to more deposition on and around it. The feedback process then recurs in another place along the river, eventually leading to the formation of braided planforms. Ashmore (1991) observed that the mechanism of middle bar formation is restricted to the near-threshold flow conditions (that is, the Shields parameter  $\Theta$  is in the order of 0.06).



**Fig. 9.14** Photograph of a middle bar in a river (courtesy of A. Radecki-Pawlik, Polish Academy of Sciences, Poland)

The mechanism therefore involves the deposition of coarser particles carried as a bed load by the stream flow, where a small change of local flow depth can be adequate to reduce the local bed shear stress below the threshold bed shear stress, being incompetent to transport the coarser particles. Figure 9.14 displays a photograph of a middle bar in a river.

In an experimental study, Ashmore (1991) observed that another kind of bar formation process, called the *transverse bar conversion*, is prevalent. The main morphological feature of a transverse bar is that it has downstream avalanche faces being developed under high stream power conditions. Initially, a contracted chute (narrow channel) with steep sides is formed due to bed erosion by the flow convergence, which possesses an enhanced stream power. Consequently, a substantial amount of sediment is removed due to the chute erosion and transported downstream. As a part of this process, as the flow diverges out of the contracted chute with a declining flow competency to carry sediment, a massive sediment load is then deposited forming an incipient bar. As the time progresses, the bed load continues to deposit in succession in the form of layers as it passes over and across the bar. This process contributes to the vertical accretion of the bar form by building up its surface. In the process of deposition of sediment, a steep slant face is formed where the deposited sediment starts to avalanche over the downstream edges of the bar. As the elevation of the bar grows, the emerging bar starts to





**Fig. 9.15** Photograph of a transverse bar in a river (courtesy of A. Radecki-Pawlik, Polish Academy of Sciences, Poland)



**Fig. 9.16** Photograph of the chute cutoff of a point bar in a river (courtesy of A. Radecki-Pawlik, Polish Academy of Sciences, Poland)

obstruct the flow that is then deflected off the edges of the bar. The mechanism of middle bar formation is thus different from that of transverse bar, where the bar accretions are initiated by the erosion and extensive deposition of large amount of bed load, rather than the deposition of only the coarser sediment particles which are locally incompetent to transport by the flow. In contrast to middle bars, when the bed shear stress is considerably greater than its threshold value, it is possible for the large amount of sediment required for the transverse bar mechanism to be eroded and deposited (Ashmore 1991). Figure 9.15 shows a photograph of a transverse bar in a river.





**Fig. 9.17** Photograph of a dissected bar in a river (courtesy of A. Radecki-Pawlik, Polish Academy of Sciences, Poland)

According to Ashmore (1991), other two mechanisms involved in the formation of a braid can be described as erosional processes. They are *chute cutoff* and *multiple bar dissection*. In *chute cutoff*, the development of a chute due to bed erosion across a point bar is prevalent during the inception of braiding. Eventually, the point bar is separated off from the bank (Fig. 9.16). Chute, in this case, represents a relatively narrow stream that occurs due to flow concentration to run through a point bar surface. Chute cutoff may occur on single point bars in existing braided rivers or across alternate point bars in moderately straight rivers. In a developed state, the size of chute may become almost similar to that of main stream on the other side of the separated point bar. Further, middle bars can also be cutoff by a single stream or multiple streams exhibiting *multiple bar dissection* (Rundle 1985a, b). Flow concentration is responsible to the formation of cutoff into the bar surface. The dissection of bars usually occurs during high flow stages when the flow crosses over the submerged bar surface. In low flow stages, the dissected bars are exposed as two or more in numbers of smaller bars, as shown in Fig. 9.17.

There are additional situations associated with the braid formations that need to be discussed. *Avulsion* is defined as a relatively abrupt switching of the stream flow from one branch to another (Ferguson 1993). This situation prevails when chute cutoffs form. Also it may occur when the stream flows switch over to previously abandoned branches of stream. Another mechanism includes the blocking of a stream flow by a bar deposition and thus leading to the formation of an upstream pool and a downstream overfall.

## References

- Agarwal VC (1983) Studies on the characteristics of meandering streams. PhD thesis, University of Roorkee, Roorkee
- Ashmore PE (1991) How do gravel-bed rivers braid? *Can J Earth Sci* 28(3):326–341
- Bergs MA (1989) Flow processes in a curved alluvial channel. PhD thesis, University of Iowa, Iowa City
- Bristow CS, Best JL (1993) Braided rivers: perspectives and problems. In: Best JL, Bristow CS (eds) *Braided rivers*. Geological Society of London, London pp 1–11 (Special publication number 75)
- Carson MA (1984) The meandering-braided river threshold: a reappraisal. *J Hydrol* 73(3–4):315–334
- Carson MA (1986) Characteristics of high-energy ‘meandering’ rivers: the Canterbury Plains, New Zealand: part one. *NZ Geogr* 40:12–17
- Carson MA, Griffiths GA (1987) Bedload transport in gravel channels. *New Zealand J Hydrol* 26(1):1–115
- Carson MA, Lapointe MF (1983) The inherent asymmetry of river meander planform. *J Geol* 91(1):41–55
- Chang HH (1988) *Fluvial processes in river engineering*. Wiley, New York
- Chatley H (1938) Hydraulics of large rivers. *J Junior Inst Eng* 48:401–416
- Dietrich WE, Smith JD (1983) Influence of the point bar on flow through curved channels. *Water Resour Res* 19(5):1173–1192
- Dietrich WE, Smith JD (1984) Bedload transport in a river meander. *Water Resour Res* 20(10):1355–1380
- Eakin HM (1910) The influence of the earth’s rotation upon the lateral erosion of streams. *J Geol* 18(5):435–447
- Einstein A (1926) The cause of the formation of meanders in the courses of rivers and of the so-called Baer’s law. *Die Naturwissenschaften* 14:1–3
- Ferguson RI (1987) Hydraulic and sedimentary controls of channel pattern. In: Richards KS (ed) *River channels: environment and process*. Basil Blackwell, Oxford, pp 129–158
- Ferguson RI (1993) Understanding braiding processes in gravel-bed rivers: progress and unsolved problems. In: Best JL, Bristow CS (eds) *Braided rivers*, Geological Society of London, London, pp 73–87 (Special publication number 75)
- Friedkin JF (1945) Laboratory study of the meandering of alluvial rivers. United States Waterways Experiment Station, Vicksburg
- Gagliano SM, Howard PG (1984) The neck cutoff oxbow lake cycle along the lower Mississippi river. In: Elliot CM (ed) *River meandering*. American Society of Civil Engineers, New York, pp 147–158
- Garde RJ, Ranga Raju KG (2000) *Mechanics of sediment transportation and alluvial stream* probable. New Age International Publishers, New Delhi
- Gay GR, Gay HH, Gay WH, Martinson HA, Meade RH, Moody JA (1998) Evolution of cutoffs across meander necks in Powder River, Montana, United States of America. *Earth Surf Proc Land* 23(7):651–662
- Gilbert GK (1884) The sufficiency of terrestrial rotation for the deflection of streams. *Am J Sci* 162:427–432 (Memories of the National Academy of Sciences, Series 3, Part 1)
- Griggs RF (1906) The Buffalo River: an interesting meandering stream. *Bull Geol Soc Am* 38(3):168–177
- Hayashi T, Ozaki S (1978) Alluvial bed form analysis I, formation of alternating bars and braids. In: *Proceedings of the United States-Japan bi-national seminar on erosion and sedimentation, Hawaii*, pp 7.1–7.39
- Henderson FM (1963) Stability of alluvial channels. *Trans Am Soc Civ Eng* 128:657–686
- Hjulström F (1957) A study of the meander problem. Bulletin 51, Institute of Hydraulics, Royal Institute of Technology, Stockholm

- Hooke JM (1995) River channel adjustment to meander cutoffs on the River Bollin and River Dane, northwest England. *Geomorphology* 14(3):235–253
- Ikeda S, Nishimura T (1985) Bed topography in bends of sand-silt rivers. *J Hydraul Eng* 111(11):1397–1411
- Ikeda S, Nishimura T (1986) Flow and bend profile in meandering sand-silt rivers. *J Hydraul Eng* 112(7):562–579
- Ikeda S, Parker G, Sawai K (1981) Bend theory of river meanders, part 1. Linear development. *J Fluid Mech* 112:363–377
- Ikeda S, Tanaka M, Chiyoda M (1985) Turbulent flow in a sinuous air duct. In: *Proceedings of the international symposium on refined flow modelling and turbulence measurements*. International Association for Hydraulic Research, The University of Iowa, Iowa City, pp 124.1–124.10
- Inglis CC (1947) Meanders and their bearing on river training. *Maritime and Waterways Engineering Division, The Institution of Civil Engineers, London*, pp 1–54
- Kikkawa H, Ikeda S, Kitagawa A (1976) Flow and bed topography in curved open channels. *J Hydraul Div* 102(9):1327–1342
- Lacey JM (1923) Some problems connected with rivers and canals in southern India. *Minutes Proc Inst Civ Eng (London)* 216(2):150–160
- Lane EW (1957) A study of the shape of channels formed by natural streams flowing in erodible material. United States Army Engineer Division, Missouri River Division, Corps of Engineers, Omaha, Nebraska
- Langbein WB, Leopold LB (1966) River meanders—theory of minimum variance. Professional paper 422-H, United States Geological Survey, Washington, DC, pp H1–H15
- Leliavsky S (1966) An introduction to fluvial hydraulics. Dover, New York
- Leopold LB, Wolman MG (1957) River channel patterns: braided, meandering and straight. Professional paper 282-B, United States Geological Survey, Washington, DC
- Leopold LB, Wolman MG (1960) River meanders. *Bull Geol Soc Am* 71:769–794
- Millar RG (2000) Influence of bank vegetation on alluvial channel patterns. *Water Resour Res* 36(4):1109–1118
- Neu HA (1967) Transverse flow in a river due to earth's rotation. *J Hydraul Div* 93(5):149–165
- Odgaard AJ (1989) River-meander model. I: development. *J Hydraul Eng* 115(11):1433–1450
- Onishi Y, Jain SC, Kennedy JF (1976) Effects of meandering in alluvial streams. *J Hydraul Div* 112(7):899–917
- Parker G (1976) On the causes and characteristic scales of meandering and braiding in rivers. *J Fluid Mech* 76:457–480
- Parker G (1979) Hydraulic geometry of active gravel rivers. *J Hydraul Div* 105(9):1185–1201
- Parker G (1984) Discussion of 'lateral bed load transport on side slopes'. *J Hydraul Eng* 110(2):197–203
- Parker G, Diplas P, Akiyama J (1983) Meander bends of high amplitude. *J Hydraul Eng* 109(10):1323–1337
- Prus-Chacinski TM (1954) Patterns of motion in open-channel bends. *Int Assoc Sci Hydrol* 383:311–318
- Quraishy MS (1943) River meandering and the earth's rotation. *Current Sci* 12:278
- Ramette M (1980) A theoretical approach on fluvial processes. In: *First international symposium on river sedimentation*, Beijing, pp C16.1–C16.18
- Ripley HC (1927) Relation of depth to curvature of channels. *Trans Am Soc Civ Eng* 90:207–238
- Robert A (2003) River processes: an introduction to fluvial dynamics. Arnold, London
- Rozovskii IL (1957) Flow of water in bends in open channels. Academy of Sciences of the Ukrainian Soviet Socialist Republic, Kiev
- Rundle A (1985a) The mechanism of braiding. *Z Geomorphol* 55(Supplement-Band):1–13
- Rundle A (1985b) Braid morphology and the formation of multiple channels. *Z Geomorphol* 55(Supplement-Band):15–37
- Schoklitsch A (1937) Hydraulic structures, vol 1. American Society of Mechanical Engineers, New York

- Shen HW (1983) Examination of present knowledge of river meandering. In: Elliot CM (ed) River meandering. In: Proceedings of the conference Rivers-83, American Society of Civil Engineers, New York, pp 1008–1012
- Simons DB, Sentürk F (1977) Sediment transport technology. Water Resources Publication, Fort Collins
- Southard JB, Smith ND, Kuhnle RA (1984) Chutes and lobes: newly identified elements of braiding in shallow gravelly streams. In: Koster EH, Steel RJ (eds) Sedimentology of gravels and conglomerates. Canadian Society of Petroleum Geologists, Calgary, pp 51–59 (Memoir 10)
- Vanoni VA (1975) Sedimentation engineering. ASCE manual number 54, American Society of Civil Engineers, New York
- von Schelling H (1951) Most frequent particle paths in a plane. *Trans Am Geophys Union* 32(2):222–226
- Werner PW (1951) On the origin of river meanders. *Trans Am Geophys Union* 32(6):898–902
- Yalin MS, da Silva AMF (2001) Fluvial processes. IAHR Monograph, International Association for Hydraulic Research, Delft
- Yang CT (1971) On river meanders. *J Hydrol* 13(3):231–253
- Zeller J (1967) Meandering channels in Switzerland. In: Proceedings of the symposium on river morphology, International Association of Scientific Hydrology, vol 75. Bern, pp 174–186
- Zimmermann C, Kennedy JF (1978) Transverse bed slopes in curved alluvial streams. *J Hydraul Div* 104(1):33–48

Fluvial Hydrodynamics

Hydrodynamic and Sediment Transport Phenomena

Dey, S.

2014, XXXII, 687 p. 254 illus., 203 illus. in color.,

Hardcover

ISBN: 978-3-642-19061-2